Monthly Notices
of the
ROYAL ASTRONOMICAL SOCIETY

MNRAS **492,** 3657–3661 (2020)
Advance Access publication 2020 January 11

doi:10.1093/mnras/staa068

Evolution of MAXI J1631–479 during the January 2019 outburst observed by *INTEGRAL*/IBIS

M. Fiocchi [1★] F. Onori [1★] A. Bazzano,[1★] A. J. Bird [2] A. Bodaghee,[3] P. A. Charles,[2] V. A. Lepingwell,[2] A. Malizia,[4] N. Masetti,[4,5] L. Natalucci[1] and P. Ubertini[1]

[1]*Istituto di Astrofisica e Planetologia Spaziali (INAF), Via Fosso del Cavaliere 100, Roma, I-00133, Italy*
[2]*Department of Physics & Astronomy, University of Southampton, Highfield, Southampton, SO17 1BJ, UK*
[3]*DCPA Georgia College Milledgeville, GA, USA*
[4]*INAF-Osservatorio di Astrofisica Spaziale e Scienza dello Spazio, via Gobetti 93/3, I-40129, Bologna, Italy*
[5]*Departamento de Ciencias Físicas, Universidad Andrés Bello, Fernández Concha 700, Las Condes, Santiago, Chile*

Accepted 2020 January 6. Received 2019 December 12; in original form 2019 June 27

ABSTRACT

We report on a recent bright outburst from the new X-ray binary transient MAXI J1631–479, observed in January 2019. In particular, we present the 30–200 keV analysis of spectral transitions observed with *INTEGRAL*/IBIS during its Galactic plane monitoring program. In the MAXI and BAT monitoring period, we observed two different spectral transitions between the high/soft and low/hard states. The *INTEGRAL* spectrum from data taken soon before the second transition is best described by a Comptonized thermal component with a temperature of $kT_e \sim 30$ keV and a high-luminosity value of $L_{2-200\,\mathrm{keV}} \sim 3 \times 10^{38}$ erg^{-1} (assuming a distance of 8 kpc). During the second transition, the source shows a hard, power-law spectrum. The lack of high energy cut-off indicates that the hard X-ray spectrum from MAXI J1631–479 is due to a non-thermal emission. Inverse Compton scattering of soft X-ray photons from a non-thermal or hybrid thermal/non-thermal electron distribution can explain the observed X-ray spectrum although a contribution to the hard X-ray emission from a jet cannot be determined at this stage. The outburst evolution in the hardness-intensity diagram, the spectral characteristics, and the rise and decay times of the outburst are suggesting that this system is a black hole candidate.

Key words: radiation mechanisms: non-thermal – stars: black holes – stars: individual: MAXI J1631–479 – stars: neutron – X-rays: binaries.

1 INTRODUCTION

In recent years, with the advent of new space and ground-based facilities, numerous efforts have been made to understand the X-ray emission in transient X-ray binaries, containing either a neutron star (NS) or a black hole (BH). These systems are characterized by transitions between two main spectral states: the high/soft state, with the dominant soft X-ray emission originating from the accretion disc, and the low/hard state, where the dominant hard X-ray emission arises from the Inverse Compton scattering of soft thermal photons by hot electrons in the corona (Done, Gierliński & Kubota 2007). The evolution of the spectral and timing properties is crucial to understand the accretion–ejection connection during an outburst for both BH and NS systems. The evolution of an outburst is well described in the hardness-intensity diagram, which represents a useful tool to investigate on the phenomenological connections between the spectral-timing states and the outflows modes (Fender 2004; Fender, Belloni & Gallo 2004; Done et al. 2007; Fender & Belloni 2012; Belloni & Motta 2016; Fender 2016; Belloni 2018; Gardenier & Uttley 2018, and references therein). Although the geometry of these systems is fairly well established, the jet contribution to the high energy emission in the hard state is still unclear.

A new outburst from MAXI J1631–479 was reported on 2018 December 21 by the *MAXI/GSC* nova alert system reporting a bright hard X-ray outburst in the Norma region (Kobayashi et al. 2018). The X-ray flux was $F_{4-10\,\mathrm{keV}} = 209 \pm 27$ mCrab at the inferred position of R.A. (J2000) = 247.770 deg., DEC (J2000) = −47.920 deg., with a 90 per cent confidence error radius of 10.2′. Confirmation of MAXI J1631–479 as a new X-ray transient source was provided by *NuSTAR* observations performed on 2018 December 28 at the refined position R.A. (J2000) = 16:31:13.4, DEC (J2000) = −47:48:18 with an uncertainty of 15″.

★ E-mail: mariateresa.fiocchi@inaf.it (MF); francesca.onori@inaf.it (FO); angela.bazzano@inaf.it (AB)

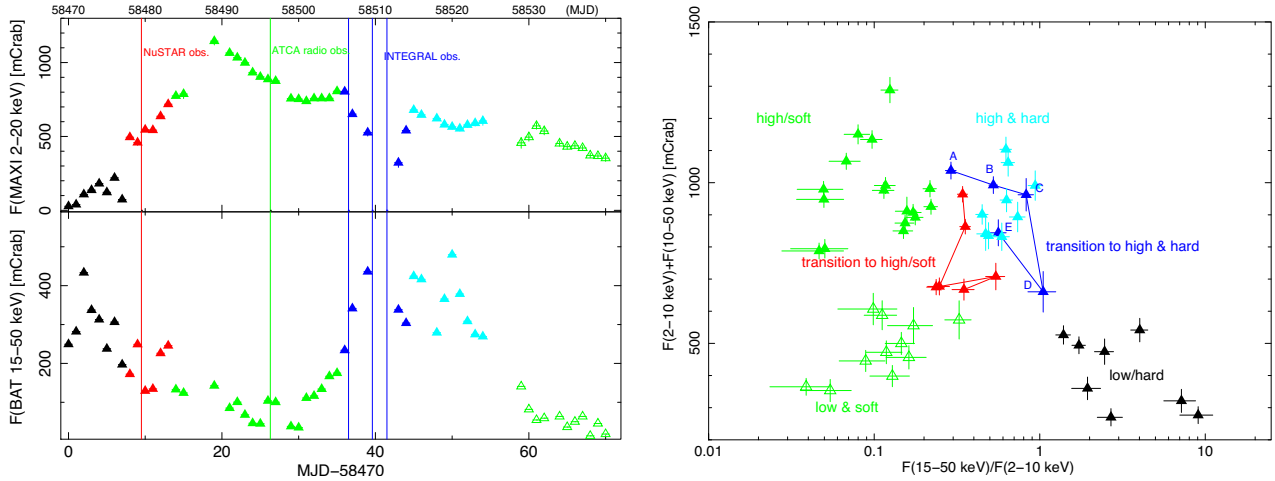

Figure 1. *Left-hand panel*: the MAXI (upper) and Swift/BAT (lower) light curves of MAXI J1631–479, both with 1-d binning. Vertical lines indicate the time of the *NuSTAR*, ATCA, and *INTEGRAL* observations. See text for details. *Right-hand panel*: the hardness-intensity diagram with each point corresponding to 1 d: on the horizontal axis, we show the ratio $F^{BAT}_{(15-50\,\mathrm{keV})}/F^{MAXI}_{(2-10\,\mathrm{keV})}$ and in the vertical axis, the total flux $F^{BAT}_{(15-50\,\mathrm{keV})} + F^{MAXI}_{(2-10\,\mathrm{keV})}$. Coloured points indicate the different time intervals. Capitals letters indicate the time evolution of the hardness-intensity data during this transition, with A being the starting of the transition and E the end.

On 2019 January 13, a radio counterpart for MAXI J1631–479 was detected by the Australia Telescope Compact Array (ATCA) observations at central frequencies of 5.5 and 9 GHz (Russell, van den Eijnden & Degenaar 2019). A clear identification of an optical counterpart is missing, consistently with the high column density found in the *NuSTAR* observation. Indeed, the position of MAXI J1631–479 was observed with KMTNet telescopes (Kim et al. 2016), with the iTelescope.Net T17 and with the 1m telescope of the CHILESCOPE observatory (Kong 2019) and no new optical source was clear found at the position of the radio detection (Shin et al. 2019).

INTEGRAL started Norma region observations as part of the Galactic plane scan in revolution 2048 (2019 January 21–23) and MAXI J1631–479 was clearly detected by *IBIS*/ISGRI (Onori et al. 2019). The position of the source in the 22–60 keV energy band was R.A. (J2000) = 247.814 deg, DEC (J2000) = −47.800 deg with an error radius of 0.5′ and a flux $F_{22-60\,\mathrm{keV}} = 265.2 \pm 3.7$ mCrab. Here, we report the results from our analysis of the *IBIS*/ISGRI data up to 200 keV.

2 OBSERVATIONS AND DATA ANALYSIS

MAXI J1631–479 has been monitored at high energies by *INTEGRAL* during three revolutions: 2048, 2049, and 2050, starting from 2019-01-21T13:30 UTC (58504.563 MJD), 2019-01-24T02:47 UTC (58507.117 MJD), and 2019-01-26T19:12 UTC (58509.801 MJD), respectively.

The *INTEGRAL*/IBIS (Ubertini et al. 2003) consolidated data for these observations were processed using the standard Offline Scientific Analysis (`osa` v11.0) software, released by the *INTEGRAL* Science Data Centre (Courvoisier et al. 2003). This software was used to obtain both spectra and light curves of the source in different common time intervals and a systematic error of 2 per cent was included. MAXI J1631–479 was out of the JEM-X field of view and this precludes INTEGRAL detection at lower energies (<30 keV).

The Neil Gehrels *Swift* observatory (Gehrels et al. 2004) collected data from this source in January 2019. We used the results from *BAT* (Krimm et al. 2013) observations, while the XRT (Burrows et al. 2004) data are not simultaneous with the *INTEGRAL* ones. In view of the strong variability of the source, a common *INTEGRAL*-Swift spectral study in a broad energy band is not possible.

MAXI J1631–479 was also observed by the Monitor of All-sky X–ray Image (Matsuoka et al. 2009), and their data have been used in our analysis.

We use `xspec` v12.10.1 (Arnaud 1996) in order to fit each spectral state in the 30–200 keV energy range.

3 SPECTRAL ANALYSIS RESULTS

In order to study the hard X-ray spectral properties of MAXI J1631–479, we analyse the *INTEGRAL*/IBIS data taken during the three *INTEGRAL* revolutions, over the energy range 30–200 keV.

The time evolution and the respective behaviour of the different spectral states are shown in Fig. 1, where the 1-d binned light curves from MAXI[1] and *Swift*/BAT[2] are reported. The variation of the source along the outbursts is clearly visible from these light curves. The epochs of the *NuSTAR* (red line), ATCA (green line), and *INTEGRAL* (blue line) observations are shown for comparison. The flux conversion into mCrab was obtained with the following factors: 1mCrab ∼ 0.00022 ct cm^{-2} s^{-1} and 1Crab ∼ 3.8 ph cm^{-2} s^{-1} for *Swift*/*BAT* [1] and *MAXI*/*GSC* [2], respectively.

Although the source is within the *BAT* confusion radius of another X-ray transient, namely AX J1631.9 − 4752, the *MAXI*/*GSC* light curve is not contaminated significantly. Indeed, during the monitoring period, while MAXI J1631–479 is detected at high flux levels, AX J1631.9 − 4752 is continuously detected at low level by *Swift*/*BAT*. The lack of contamination is confirmed by the *INTEGRAL*/IBIS map, where the emission from AX J1631.9 − 4752 is lower than ∼10 mCrab (3σ upper limit) in the 30–50 keV energy range.

We performed an analysis for spectral variability by plotting the hardness versus total emission in two energy bands.

[1] *http://MAXI/GSC.riken.jp/top/slist.html*
[2] *https://swift.gsfc.nasa.gov/results/transients*

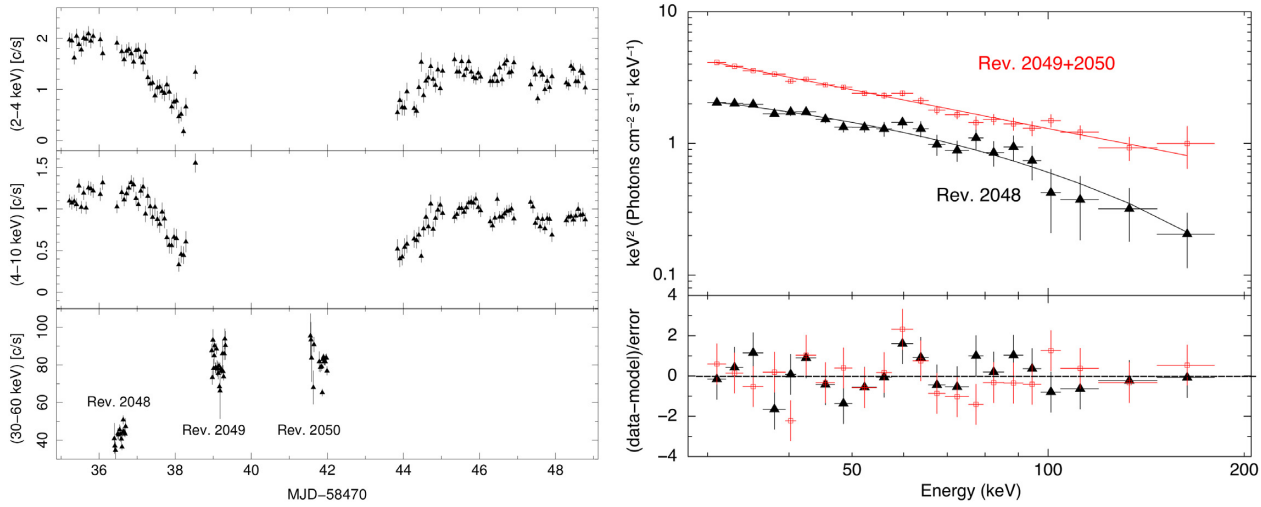

Figure 2. *Left-hand panel*: Zoomed-in light curves during the *INTEGRAL* observation period, with the top (2–4 keV) and middle (4–10 keV) *MAXI/GSC* light curves (in 6-h bins, data from *http://maxi.riken.jp/top/slist.html*) compared with the bottom (30–60 keV) IBIS light curve (in 2000-s bins) over the three *INTEGRAL* revolutions. *Right-hand panel*: *INTEGRAL*/IBIS unfolded spectra and residuals in sigma during revolution 2048 (in black) and during revolutions 2049 and 2050 (in red). Model is a cut-off power law for the first data set and a simple power law for the second one.

Fig. 1 (right-hand panel) shows the hardness-intensity diagram for the *MAXI/GSC* and *Swift*/*BAT* observations. The hardness is derived using the ratio between the fluxes in these two X-ray bands $F^{BAT}_{(15-50\,\mathrm{keV})}/F^{MAXI}_{(2-10\,\mathrm{keV})}$ and is plotted versus the total flux $F^{BAT}_{(15-50\,\mathrm{keV})}+F^{MAXI}_{(2-10\,\mathrm{keV})}$. Each point corresponds to 1 d of time integration and only epochs for which both soft and hard X-ray data are available have been used.

The different coloured points in the right-hand panel of Fig. 1 represent six regions we have selected from the temporal intervals. These regions correspond to the different spectral states identified in the *MAXI/GSC* and *Swift*/*BAT* light curves, as shown in the left-hand panel of Fig. 1:

(i) 1st epoch: from MJD 58470 to 58478, the source shows a low flux level at soft energy and a high flux level in the hard X-ray band. This is typical behaviour for the low/hard state (black points).

(ii) 2nd epoch: from MJD 58479 to 58485, the source shows an increasing soft flux and a decline in hard X-ray, indicating a transition from the low/hard state to a high/soft state (red points).

(iii) 3rd epoch: from MJD 58486 to 58506, the source shows a high soft flux level and is low in hard X-rays, indicative of a standard high/soft state (green points).

(iv) 4th epoch: from MJD 58507 to 58514, the source shows unusual variability during this period. A decline in the soft X-ray emission is observed for 3 d, followed by a sudden increase lasting for 2–3 d. Unfortunately, no soft X-ray data are available for the 2 d in between this change in the emission. In the same period, the source experienced an increase in hard X-rays corresponding to a soft X-ray decline, followed by a slight drop in hard flux with a corresponding enhancement in soft X-rays. This behaviour suggests that during the first 3 d, the source started a transition from the high/soft state to a low/hard state. Afterwards, it suddenly reversed this trend towards a new state (blue points).

(v) 5th epoch: from MJD 58515 to 58522, the source shows a high flux level in both soft and hard bands. This suggests that in this epoch, MAXI J1631–479 can be considered being in an intermediate state (light blue points), where the X-ray emission can be explained with hybrid (thermal and non-thermal) Comptonization models.

(vi) 6th epoch: from MJD 58529 to 58540, the source transits towards a soft state at low luminosity level (green empty points).

The IBIS/*INTEGRAL* observations occurred during the 4th epoch and fall in the region of the blue points in the right-hand panel of Fig. 1 and marked as blue vertical lines in the left-hand panel, for comparison. The IBIS observations carried out during revolution 2048 fall close in time to the first *MAXI/GSC* blue point (point A in Fig. 1, right-hand panel). No *MAXI/GSC* and *BAT* simultaneous data are available for the second and third IBIS/*INTEGRAL* observations.

The left-hand panel of Fig. 2 shows the 2–4 keV and 4–10 keV MAXI light curves (bin time 6 h), together with the 30–60 keV IBIS light curve (bin time 2000 s). The variation in the source spectral state during the *INTEGRAL* observation is clearly visible. In particular, during the first *INTEGRAL*/IBIS observation (revolution 2048), the source is in a high/soft state; however, during the subsequent observations (revolutions 2049 and 2050), the source flux increased by a factor of ∼2 in the 30–60 keV energy range, indicating the occurrence of the transition to a low/hard state.

We performed spectral analysis for the three *INTEGRAL* revolutions separately.

First, we attempted to fit the spectra using a simple power-law model. For the spectrum of revolution 2048, we obtain a spectral index of 3.1 ± 0.1 and a χ^2/degrees of freedom of 34/20, with residuals at high energies. Then we modelled these data with a cut-off power-law, which resulted in a best-fit with χ^2/degrees of freedom = 25/19. In this case, we obtain a spectral index $\Gamma = 2.1^{+0.6}_{-0.5}$, $E_{\mathrm{cutoff}} = 62^{+20}_{-22}$ keV and a high energy flux of $F_{30-200\,\mathrm{keV}} = (2.8 \pm 0.1) \times 10^{-9}$ erg cm^{-2} s^{-1}. However, we remark that by using the latter model, the fit improvement is only marginal. Indeed, applying the appropriate *F*-test statistics for model comparison (Press et al. 2007; see also Orlandini et al. 2012), we obtain an improvement probability of only about 28 per cent.

In order to obtain the physical parameters of the source, we also fit this data set using a model describing the Comptonization of soft photons in a hot plasma (`comptt` in `xspec`, Titarchuk 1994). The resulting Comptonized plasma has a temperature of ∼29 keV and optical depth $\tau \sim 0.7$, with the input soft photon Wien temperature fixed at the default value (0.1 keV), not affecting the high energy

Table 1. Spectral results of the IBIS/INTEGRAL observations.

Model	Parameter	Rev. 2048	Rev. 2049 + 2050
		IBIS exposure	
		13 ks	36 ks
Power law	Γ	3.1 ± 0.1	2.98 ± 0.04
	$F^{a}_{30-200\,keV}$	3.0 ± 0.1	5.9 ± 0.1
	χ^2/degrees of freedom	34/20	20/20
Cutoff	Γ	$2.1^{+0.6}_{-0.5}$	...
Power law	E_{cutoff} (keV)	62^{+20}_{-22}	...
	$F^{a}_{30-200\,keV}$	2.8 ± 0.1	...
	χ^2/degrees of freedom	25/19	...
Comptt	kT_e (keV)	29^{+43}_{-10}	...
	τ	0.7 ± 0.4	...
	$F^{a}_{30-200\,keV}$	2.9 ± 0.1	...
	χ^2/degrees of freedom	25/19	...

[a]Flux in units of 10^{-9} erg cm^{-2} s^{-1}.

spectrum. The best-fitting parameters are listed in Table 1. In the right-hand panel of Fig. 2, the spectrum of revolution 2048, together with residuals with respect to the cut-off power-law model, is shown (black filled triangles).

When fitting the IBIS data of revolutions 2049 and 2050 separately, we obtain similar results, both in flux and in spectral shape. This is also evident from Fig. 1 (right-hand panel), where IBIS observations fall in the same hardness region (between points C and D). Using a simple power-law model, we obtain a spectral index of 3.0 ± 0.2, a flux of $F_{30-200\,keV} = (5.9 \pm 0.2) \times 10^{-9}$ erg cm^{-2} s^{-1} and a χ^2/degrees of freedom of 20/20 for revolution 2049 and for revolution 2050 ($\Gamma = 3.0 \pm 0.2$, a flux of $F_{30-200\,keV} = (5.9 \pm 0.2) \times 10^{-9}$ erg cm^{-2} s^{-1} and a χ^2/degrees of freedom of 20/20). No high energy cutoff is required for these data. Taking into account the spectral similarity, similar flux levels, and hardness, data from revolutions 2049 and 2050 have been combined to improve the statistical quality of the spectra and to better constrain the physical parameters, as reported in Table 1. The resulting spectrum together with the residuals with respect to the power-law model is shown in Fig. 2 with red squares (right-hand panel).

4 DISCUSSION

MAXI J1631–479 belongs to a class of transient systems showing spectral state transitions.

When it starts to transit towards a hard state (Negoro et al. 2019), the *INTEGRAL*/IBIS observation shows that the source had a high X-ray flux $F_{30-200\,keV} \sim 3 \times 10^{-9}$ erg cm^{-2} s^{-1}and a hard spectrum (blue lines of Fig. 1, at ∼58506 MJD) and it is dominated by a hard X-ray Comptonized component, arising from inverse Compton scattering of soft thermal photons in a hot corona with $kT_e \sim 29$ keV and $\tau \sim 0.7$.

This intermediate value of the electron temperature confirms that the source is not in a standard high/soft or low/hard state. Joinet et al. (2008) found a similar corona temperature (∼30 keV) when the microquasar GRO J1655–40 transits from low/hard to hard/intermediate state. This temperature of the thermal population was also previously observed in GX 339-4 [Motta, Belloni & Homan (2009)] before the source transits from low/hard to hard/intermediate state. In this case, the high energy cutoff disappears near the hard/intermediate–soft/intermediate transition. This behaviour is similar to the MAXI J1631–479 evolution: the high energy cutoff was not detected by *INTEGRAL*/IBIS when it moved towards a soft state at low luminosity. Indeed, it is detected up to about 200 keV though the best fit is a simple power law ($\Gamma \sim 3$), suggesting a non-thermal origin for this X-ray emission. This behaviour continued in later observations, as noted in Fig. 1, where the light blue points show that the source moved towards an intermediate state at a high flux in both soft and hard bands.

Transitions from low/hard state to high/soft state and then towards an intermediate state with high flux at these energies have previously been observed in BH systems (Done et al. 2007; Belloni 2018). The no-detection of a high energy cutoff using X-ray data up to 200 keV suggests that the hard X-ray emission may not be produced by thermal Comptonization. The observed spectrum in the intermediate state can be produced by Compton scattering on a non-thermal electron population (Gilfanov 2010) or by a mixture of thermal and non-thermal features (Coppi 1999; Del Santo et al. 2008). The shape of the hysteresis diagram of MAXI J1631–479 appears similar to the one of the BH X-ray binary XTE J1550–564 (Russell et al. 2010). Moreover, MAXI J1631–479 showed radio emission at 5.5 and 9 GHz when it was in the high/soft state (Russell et al. 2019) and a similar behaviour was reported for XTE J1550–564. For that system, the authors were able to isolate the non-thermal emission from the jet and demonstrated that the synchrotron jet may dominate in hard X-ray when the source fades in the low/hard state at very low-luminosity level. In this case, the jet produces ∼100 per cent of the emission when the soft (3–10 keV) and hard (100–250 keV) fluxes are comparable.

In the case of MAXI J1631–479, Fig. 2 shows that X-ray power-law component is observed when the soft and hard fluxes are comparable, although the energy ranges are slightly different from those used for XTE J1550–564.

Unfortunately, for this source neither the distance nor the mass of the central object is known. In order to estimate the possible luminosity range of MAXI J1631–479, we used the extreme values of distances and masses known so far for X-ray binaries. In particular, the distances span from 1 kpc (McClintock & Remillard 1986) to 27 kpc (Casares et al. 2004), while the BH masses can assume values from 4 $M_\odot$ (Özel et al. 2010) to 15.65 $M_\odot$ (McClintock & Remillard 1986; Orosz et al. 2007). Using realistic values for a LMXB, the luminosity of MAXI J1631–479 during the intermediate state can vary from 5×10^{-1} L_{Edd} (distance = 20 kpc and mass = 4 $M_\odot$) to 3.5×10^{-4} L_{Edd} (distance = 2 kpc and mass = 15.65 $M_\odot$). Thus, as the emission of the jet in X-ray band can be dominant when the luminosity is between $L \sim 2 \times 10^{-3}$ L_{Edd} and $L \sim 2 \times 10^{-4}$ L_{Edd} (Russell et al. 2010), the wide range of possible values derived for the luminosity of MAXI J1631–479 does not allow us to exclude a contribution of the jet to the X-ray emission in MAXI J1631–479.

The lack of a high energy cut-off indicates that the X-ray emission from MAXI J1631–479 has a non-thermal origin that can be produced either by Comptonization of non-thermal electron population or by a hybrid thermal/non-thermal electron distribution. The source outburst evolution and the typical times of the outburst suggest the BH nature of this source. Indeed, assuming the time spent to reach from 10 per cent to 90 per cent of the flux peak as the rise time and the reverse for the decay time, we obtained τ_{rise} ∼15 d and τ_{decay} ≥50 d though it seems that the outburst has not yet ended (see Fig. 1, left-hand panel). These values are compatible with decay and rise times for BH and incompatible with much faster evolution times for NS, reported in the statistical study of Yan & Yu (2015). This result is in agreement with previous studies performed at different energy bands during the same outburst. When MAXI

J1631–479 transits from a low/hard to high/soft state (red line of Fig. 1, ∼58480 MJD), the *NuSTAR* 3–79 keV spectrum is well modelled by a disc-blackbody with a temperature of ∼1.12 keV, a power-law with a photon index of ∼2.39, and iron Kα emission line with an equivalent width of ∼90 eV (Miyasaka et al. 2018). Based on these spectral characteristics, the authors suggested the system as a BH binary in the high/soft state, with most of the flux in the soft X-ray band ($F_{2-10\,\mathrm{keV}} = 1.7 \times 10^{-8}$ erg cm^{-2} s^{-1} and $F_{3-79\,\mathrm{keV}} = 1.8 \times 10^{-8}$ erg cm^{-2} s^{-1}). Russell et al. (2019) also report a similar conclusion on the source nature by using the radio observation performed on 2019 January 13 (green line of Fig. 1, ∼58496 MJD). A radio counterpart of MAXI J1631–479 was detected by ATCA with a flux density of $F_{5.5\,\mathrm{GHz}} = (630 \pm 50)$ μJy and a radio luminosity $L_{5\,\mathrm{GHz}} = (9.5 \pm 0.8) \times 10^{28}$ (d/5 kpc)^2 erg s^{-1}.

This radio emission could indicate the presence of a compact jet, as it was detected during the transition from high/soft to low/hard state, i.e. when synchrotron jet emission could become dominant at X-ray wavelengths and at low luminosities.

ACKNOWLEDGEMENTS

The authors acknowledge the ASI financial/programmatic support via ASI-INAF agreement number 2013-025.R1 and ASI/INAF n.2017-14-H.0.

FO acknowledge the support of the H2020 European Hemera program, grant agreement No 730970.

This research has made use of the *MAXI/GSC* data provided by RIKEN, JAXA, and the *MAXI/GSC* team.

*Swift/BAT*transient monitor results provided by the *Swift/BAT*team.

PAC is grateful to the Leverhulme Trust for the award of an Emeritus Fellowship.

Finally, the authors thank the anonymous referee for the valuable comments that helped to improve the manuscript.

REFERENCES

Arnaud K. A., 1996, in Jacoby G. H., Barnes J., eds, ASP Conf. Ser. Vol. 101, Astronomical Data Analysis Software and Systems V, Astron. Soc. Pac., San Francisco, p. 17

Belloni T. M., 2018, preprint (arXiv:1803.03641)

Belloni T. M., Motta S. E., 2016, in Bambi C., ed., Astrophysics and Space Science Library, Vol. 440, Astrophysics of Black Holes: From Fundamental Aspects to Latest Developments, Springer-Verlag, Berlin, p. 61

Burrows D. N. et al., 2004, in Flanagan K. A., Siegmund O. H. W., eds, Proc. SPIE Conf. Ser. Vol. 5165, X-Ray and Gamma-Ray Instrumentation for Astronomy XIII. SPIE, Bellingham, p. 201

Casares J., Zurita C., Shahbaz T., Charles P. A., Fender R. P., 2004, ApJ, 613, L133

Coppi P. S., 1999, in Poutanen J., Svensson R., eds, ASP Conf. Ser. Vol. 161, High Energy Processes in Accreting Black Holes. Astron. Soc. Pac., San Francisco, p. 375

Courvoisier T. J.-L. et al., 2003, A&A, 411, L53

Del Santo M., Malzac J., Jourdain E., Belloni T., Ubertini P., 2008, MNRAS, 390, 227

Done C., Gierliński M., Kubota A., 2007, A&A Rev., 15, 1

Fender R., 2004, New A Rev., 48, 1399

Fender R., 2016, Astron. Nachr., 337, 381

Fender R., Belloni T., 2012, Science, 337, 540

Fender R. P., Belloni T. M., Gallo E., 2004, MNRAS, 355, 1105

Gardenier D. W., Uttley P., 2018, MNRAS, 481, 3761

Gehrels N. et al., 2004, ApJ, 611, 1005

Gilfanov M., 2010, The Jet Paradigm, Lect. Notes Phys., Vol. 794, Springer-Verlag, Berlin Heidelberg, p. 17

Joinet A., Kalemci E., Senziani F., 2008, ApJ, 679, 655

Kim S.-L. et al., 2016, J. Korean Astron. Soc., 49, 37

Kobayashi K. et al., 2018, Astron. Telegram, No. 12320

Kong A. K. H., 2019, Astron. Telegram, No. 12504

Krimm H. A. et al., 2013, ApJS, 209, 14

Matsuoka M. et al., 2009, PASJ, 61, 999

McClintock J. E., Remillard R. A., 1986, ApJ, 308, 110

Miyasaka H., Tomsick J. A., Xu Y., Harrison F. A., 2018, Astron. Telegram, No. 12340

Motta S., Belloni T., Homan J., 2009, MNRAS, 400, 1603

Negoro H. et al., 2019, Astron. Telegram, No. 12421

Onori F. et al., 2019, Astron. Telegram, No. 12418

Orlandini M., Frontera F., Masetti N., Sguera V., Sidoli L., 2012, ApJ, 748, 86

Orosz J. A. et al., 2007, Nature, 449, 872

Özel F., Psaltis D., Narayan R., McClintock J. E., 2010, ApJ, 725, 1918

Press W. H., Teukolsky S. A., Vetterling W. T., Flannery B. P., 2007, Numerical Recipes: the Art of Scientific Computing, Cambridge Univ. Press, Cambridge

Russell D. M., Maitra D., Dunn R. J. H., Markoff S., 2010, MNRAS, 405, 1759

Russell T. D., van den Eijnden J., Degenaar N., 2019, Astron. Telegram, No. 12396

Shin M.-S., Kim J.-W., Chang S.-W., Lee C.-U., Kim S.-L., 2019, Astron. Telegram, No. 12438

Titarchuk L., 1994, ApJ, 434, 570

Ubertini P. et al., 2003, A&A, 411, L131

Yan Z., Yu W., 2015, ApJ, 805, 87

This paper has been typeset from a TEX/LATEX file prepared by the author.